The Green Berries

Margy Gentile
Mini-Project
Microbial Diversity
August 1, 2002

Abstract

The microbial composition, structure, and activity of green bacterial aggregates (known as "berries") found in Sippewissett Salt Marsh was characterized by confocal microscopy, spectral analysis, microelectrode measurements, and clone libraries. The interior of these aggregates is dominated by a *Cyanthece*, a unicellular cyanobacteria. A thin, distinct layer surrounds the aggregate and is composed of non-Chlorophyll *a* containing bacteria, filamentous cyanobacteria, diatoms, and other eukaryotes. Microelectrode experiments revealed the production of oxygen within the berry during light periods and the consumption of oxygen during dark periods. Two types of *Cyanothece* aggregates, designated as light or dark green, were differentiated based upon macroscopic examination. Subsequent analysis revealed that these aggregates were composed of cells of different average cell sizes, densities, structure, and pigment composition.

Introduction

Purple and green bacterial aggregates, also known as "berries", form in the tidal pools of Sippewissett Salt Marsh. The presence and formation of the berries have intrigued students of the microbial diversity course for years. The purple berries have been dissected and studied, but the greens have yet to be characterized. This mini project explored the composition of the green berries. The objectives were to determine the microbial composition of the green berries, to explore the spatial structure of cells within the aggregate, to elucidate interactions between members of the aggregate community, and to examine the differences between green berries which had visually apparent differences in color and consistency.

Materials and Methods

Sampling

All samples were taken from the same tidal pool in the Sippewissett Salt Marsh and analyzed within one week.

Microscopy

Microscopy was done using the dissecting scope, the light microscope and confocal laser scanning microscope (CLSM). Samples for confocal microscopy were stained with the general DNA stain Sybr Green for at least one half hour before imaging. The microscope was configured to differentiate between the fluorescence from the stain and the red autofluorescence of Chlorophyll *a* containing bacteria using excitation wavelengths of 488 nm and 543 nm, respectively. Wavelengths between 475 and 525 nm were detected on one channel, color coded green. The other channel, color coded red, detected autofluorescence above 650 nm. This configuration was tested with pure

cultures of Sybr Green stained *E. coli* and *Synechococcus PCC7001*. Objective lenses Plan-Neofluar 10x/0.3, Achroplan 40x/0.8W, and C-Apochromat 63x/1.2W corr were used. The emissions spectra of individual cells were obtained with the Meta Detector operated in the Lambda Mode. Samples for spectral analysis were analyzed within hours of collection.

Microelectrodes

An oxygen microelectrode from Diamond General was used to measure oxygen concentrations in and around the berries. The probe was calibrated with a two point curve, the two points being water in equilibrium with atmospheric oxygen and the anaerobic environment at the bottom of a lab microbial mat. Berries were placed in a petri dish, covered with 10 millimeters of tidal pool water, and left under a 90 Watt incandescent light bulb at a distance of 28 cm for 30 minutes to 1 hour before measurements were taken. Two types of experiments were conducted. In nine different berries, oxygen profiles were recorded as the electrode was lowered into the berry from several millimeters above it. The distances within the berry are not accurate, because stabbing it with the electrode caused it to compress. Therefore, lowering the electrode a specified distance does not correspond to a penetration of that distance into the berry. Despite these limitations, profiles were generated as oxygen concentration versus distance into the berry. Light dark experiments were conducted in four berries. After the electrode was lowered into the berry, a box was placed over the experimental set-up excluding light for a period of time and then removed. Oxygen concentrations were measured with time during the light, dark, and light again periods.

Clone Library

A clone library of the green berries was made as a class project during the first two weeks of the course. The procedure was followed as described in the course handout. In brief, DNA was extracted using the MoBio UltraClean Soil DNA Isolation Kit and PCR amplified using the universal bacterial 8F and 1492R primers. PCR products were cloned using the Invitrogen TOPO Cloning Kit. Clone colonies were picked, inoculated into media, and sent to Mitch Sogin's lab for sequencing. Sequence data was aligned and a tree constructed using a neighbor joining method in ARB.

Results

General Observations

Green berries were first observed floating on the surface of tidal pools in Sippewissett Salt Marsh. Subsequent sampling revealed that they are also present in the sediments. They were difficult to find in the field, because they blend in with the sediments. Sorting through sediment samples brought back to the lab revealed a diversity of green berries varying in size, consistency, and color. In general, the berries are very irregular in shape, range in size from 1 to 8 mm in the longest dimension, and have an associated gooey matrix. When cut open and examined under the dissecting scope, there was no noticeable difference between the interior and exterior. Small eukaryotes were seen crawling and swimming on the outside and through the berries. Examination with

the light microscope revealed masses of coccoid cells as well as many diatoms and other unicellular eukaryotes.

The initial analysis revealed two visually distinct types of green berries. One type was characterized by a dark green color and were opaque(Figure 1). These berries were highly structured and are composed of many nodules, each nodule contained many smaller round clumps. The second distinguishable type was characterized by a much lighter green color (Figure 2). These berries were more gelatinous and even transparent in sections. The light green berries were also very irregular in shape, but the nodules comprising them were less defined than in the dark green berries. Several hypotheses were proposed to explain the different character of these two types. The differences may be due to the presence of a different species, different pigment production due to some environmental condition, or a different ratio of cells to matrix material. Further examination of these two types was preformed by confocal microscopy and spectral analysis.

Confocal Microscopy Revealed Berry Structure

Berry Interior

Several berries of both types were cut open and stained with Sybr Green. The confocal microscope with a 40x objective lens was used to examine the structure of the aggregates over these cross sections. In all of the samples examined, the interior of the aggregate was dominated by a single cell type. The cells were identified as unicellular cyanobacteria, because they appeared on both the channel detecting the general bacterial stain and in the channel detecting Chlorophyll *a* autofluorescence. Closer examination of the interior of the dark green versus light green aggregates revealed several interesting differences which are summarized in Table 1. In the dark green aggregates, the cells were a bit smaller, more coccoid, more densely packed, and organized in clumps with channels of void space (Figure 3). In the light green berries the cells were on average larger, longer in one dimension, and the spatial arrangement was more random and less dense (Figure 4).

	Average Cell Size (μm)	Average Cell Density (cells/mm^3)	Interior Structure	Exterior Layer Thickness (μm)
Dark	5.45 ± 0.46 x 4.94 ± 0.31 (n=27)	0.96 ± 0.16 (n=11)	cells clumped together creating channels of void space	10-20
Light	7.85 ± 0.26 x 4.55 ± 0.14 (n=29)	0.41 + 0.10 (n=9)	cells randomly distributed without apparent structure	5-7 (patchy)

Table 1. The properties of the internal structure of light versus dark green berries. The average cell sizes and densities are reported with 95% confidence intervals and sampling sizes.

Berry Exterior

A distinct outer layer was observed to surround the entire berry. Various Chlorophyll *a* containing organisms distinct from the cyanobacteria residing in the interior were present in this layer including diatoms, filamentous cyanobacteria, and other

as yet unidentified eukaryotes. The character of the outer layer was slightly different in the light green versus dark green berries (Table 1). In the dark green berries, the layer was much thicker and the non-Chlorophyll *a* containing bacteria were more dense withi the layer (Figure 5). A void space of about 20-60 mm was observed between the interior clusters of unicellular cyanobacteria and the external layer, although in some places the unicellular cyanobacterial clusters reached out to the surface of the aggregate. In the light green berries, the outer layer is much thinner and nonexistent in patches (Figure 6). There are less non-Chlorophyll *a* containing bacteria in this layer, and more diatoms and filamentous cyanobacteria were observed.

Berry Topography

The overall topography of the green berries was explored using a 10x objective lense. At this magnification, large scale observations were made. Well defined, roughly spherical humps were observed separated by valleys in the dark green berries. At this magnification, the exterior layer and internal unicellular cyanobacteria were visualized. In the junctions of valleys were bunches containing several extremely large, 15 μm in diameter by 70 μm in length, Chlorophyll *a* containing rods. In the green channel, several large blobs were observed over the surface of the aggregate. Examination of the cross sections revealed a weblike structures (Figure 7) which was recognized to be the gelatinous matrix. This fluorescence of the matrix could have been because it contained DNA or due to autofluorescence. A similar fluorescent matrix was observed in the purple berries in unstained samples (personal communication, Koty Sharp).

Spectral Analysis

Images taken with the Meta Detector in lambda mode were analyzed to obtain spectra of individual cells. A characteristic light green berry and a characteristic dark green berry were analyzed. The examination of three cells in three separate areas of each sample yielded nine spectra per sample. All nine spectra from a given sample had similar peaks and peak ratios, but overall intensity varied. In the dark green berry, peaks were observed at 620, 660, and 680 nm (Figure 8b) corresponding to phycocyanin, allophycocyanin and Chlorophyll *a*, respectively (Brock and Madigan, 2000). The allophycocyanin peak was larger than that of Chlorophyll *a* which is somewhat unusual (personal communication, John Waterbury). The same peaks appeared in the spectra of the cells in the light green berry as well as a small peak at 580 nm, corresponding to the presence of carotenoids (Figure 8a).

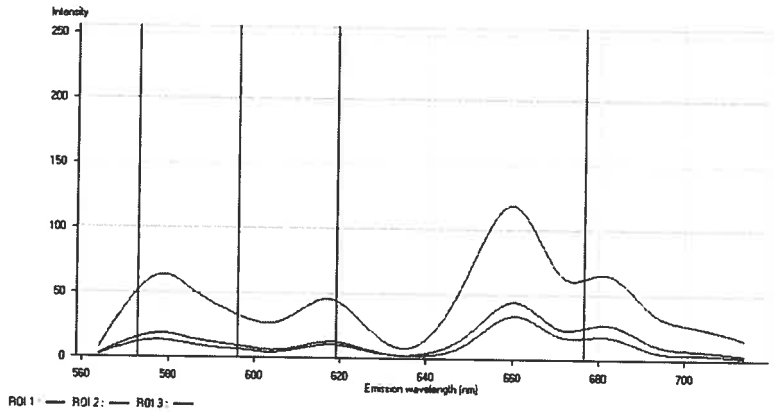

Figure 8a. Spectra of 3 cells on the interior of a light green berry.

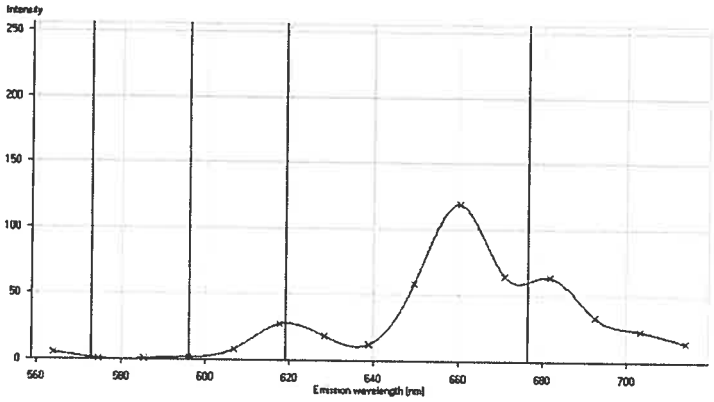

Figure 8b. Spectra of a cell on the interior of a dark green berry.

Clone Library Results

The results of the clone library are summarized in the following phylogenetic tree (Figure 9). Cyanobacteria dominated the sequences from the 69 clones analyzed. 50 of the clones clustered together within the cyanobacteria in the pylogenetic tree, although this is not shown in the abbreviated tree presented. The closest relatives to this cluster were the Mycrocystis. When these sequences were BLASTed against the NCBI database, the closest match for 50 of the sequences was *Cyanothece* with between 94 and 97 percent sequence identity. *Cyanothece* was not included in the database used to create the phylogenetic tree, so it is not surprising that it did not appear as the closest relative.

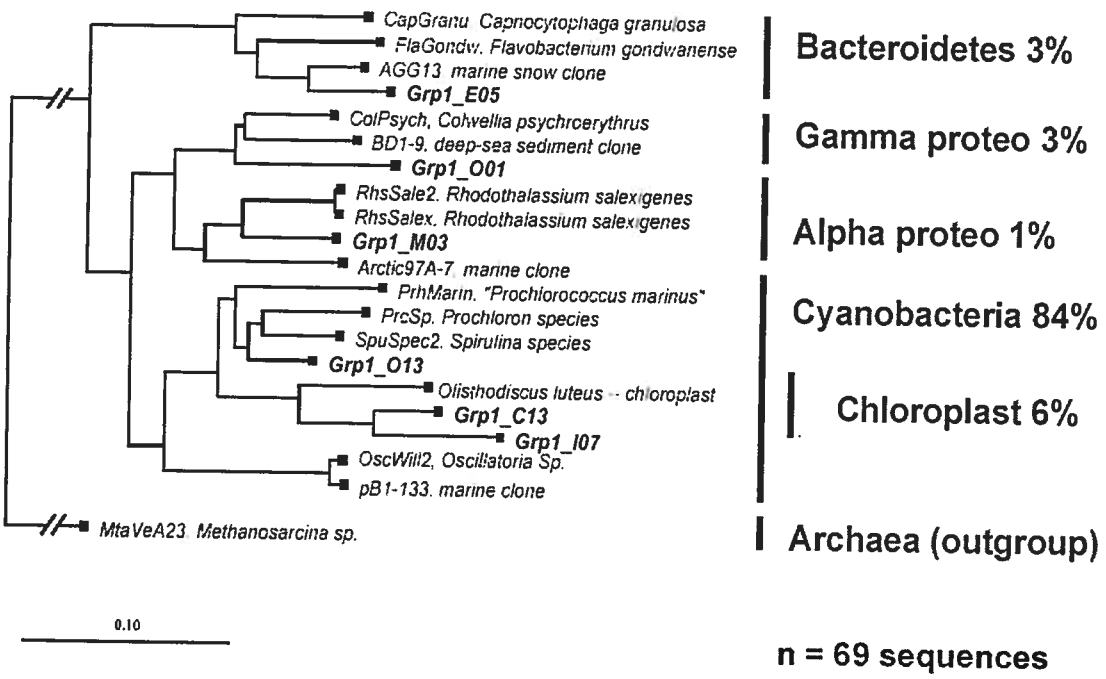

Figure 9. Phylogenetic tree of 16S rRNA sequences prepared from class data by Jeff Walker.

Further Bacterial Identification

The identification of the dominant cell type as *Cyanothece* was also consistent with the cyanobacteria identification scheme detailed in The Prokaryotes (Waterbury, 2002). The bacteria are placed into the order *Chroococcales*, because they are unicellular aggregates held together by an extracellular slime, and they appear to reproduce by binary fission in one or two planes. Further identification as *Cyanothece* is based upon a cell size of greater 3μm and the lack of a sheath. Although the cells within the light and green aggregates appeared to be growing differently, it is thought that they are both *Cyanothece* (personal communication, John Waterbury).

Microelectrode Experiments

Oxygen Profiles

Oxygen concentrations outside and inside nine green berries of various sizes from 4 to 6 mm were taken with the oxygen microelectrode. In most samples, the oxygen concentrations increased as soon as the electrode reached the surface of the berry. Figure 10 shows the results for three trials in the same berry. The oxygen concentration increased slightly before entering the berry and then increased dramatically once inside. These results are representative of those in the other berries, although in three trials oxygen concentrations decreased. However, in other trials in the same berries, the oxygen concentrations followed the behavior displayed in Figure 10. Increasing oxygen concentrations were observed in both the light and dark green berries and quantitative comparisons were not made due to the associated uncertainties with electrode penetration.

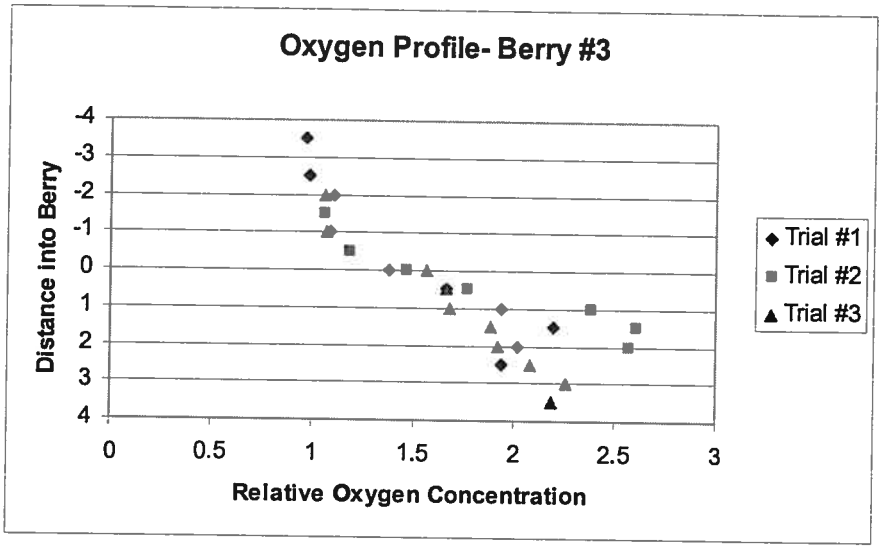

Figure 10. Representative results of an microelectrode profile experiment. Measurements were taken under light conditions. The y-axis was set to zero at the surface of the berry. The oxygen concentration is expressed as a relative value where 1 is the concentration in equilibrium with atmospheric oxygen.

Light Dark Experiments

Light dark experiments were conducted on four of the berries. The electrode was inserted into the berry and the oxygen concentration at the given position was monitored over time under light and dark conditions (Figure 11). Oxygen concentrations rapidly dropped when placed in the dark and reached zero after ten minutes in all trials, indicating oxygen consumption. The rates of consumption were comparable in all of the trials. When placed back into the light, oxygen concentrations increased, but with variable trends. During these experiments, it was observed that some berries began to float after sitting in the light for over two hours. Bubbles, presumably oxygen, were also seen on the surface of the berry. Perhaps this metabolic activity explains the floating berries observed on the surface of the tidal pools.

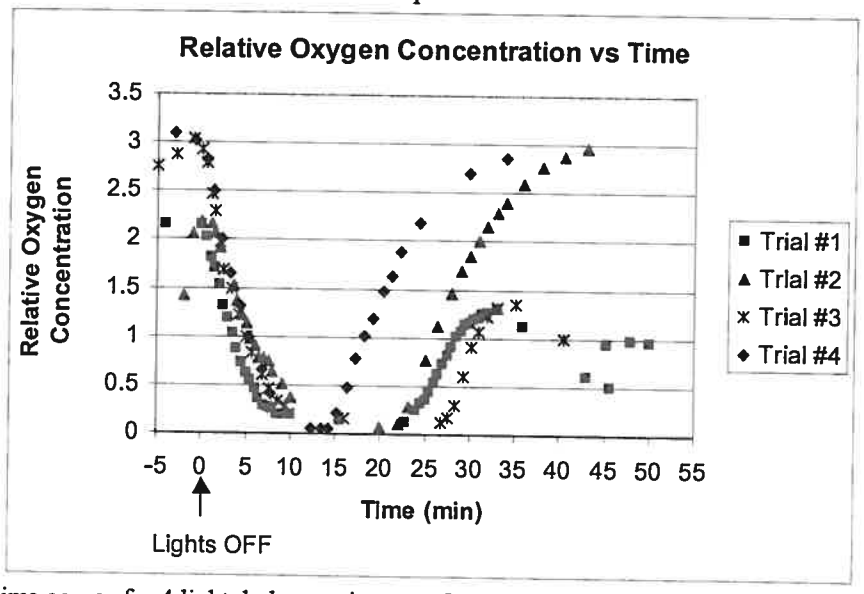

Figure 11. Time course for 4 light dark experiments. Oxygen concentrations are relative to the concentration in equilibrium with atmospheric oxygen.

Disscussion and Conclusions

The green bacterial isolates found in the tidal pools of Sippewissett Salt Marsh are comprised of a core of *Cyanothece*, a unicellular cyanobacteria, surrounded by a thin coat of other organisms. *Cyanothece* are known to produce high amounts of extracellular polysaccharides (Shah *et al.,* 2000 and Dephilippes *et al,* 1993). In one species, *Cyanothece* ATCC 51142, the EPS produced formed a gel, possibly due to precipitation at high divalent cation concentrations (Shah *et al.*, 2000). *Cyanothece* sp. 16som2 was isolated from a microbial mat near Getzira, Somaliland and was found to produce more EPS when under nitrogen limitation (Dephilippes *et al.,* 1993). Perhaps the *Cyanothece* in the green berries are experiencing nitrogen limitation or producing a gel forming EPS that could contribute to berry formation. Although the microelectrode experiments were not quantitative, they did reveal that oxygen is produced in the light and consumed in the dark. *Cyanothece* are thought to utilize large interthylakoidal carbohydrate granules to power nitrogen fixation in the dark cycle (Schneegurt *et al.*, 1996), thus accounting for the consumption of O_2 under dark conditions.

Although ultimately thought to be comprised of the same species, several interesting features were observed to differentiate the visual classifications of light green and dark green berries. The average cell size, density, spatial arrangement, and pigment composition were different in the two types. Several possible explanations for the differences arose. Perhaps the light green berries are less healthy than the dark green berries or are actually a dark green berry that is dying. Alternatively, the light green berry may be a dark green berry at an earlier stage of growth. The production of pigments is often different under nitrogen limiting conditions, so perhaps this or another environmental condition could account for the difference.

Further experiments are necessary to determine the formation and differentiation of the green berries. Culturing the *Cyanothece* in the lab might yield insights into aggregate development, EPS formation, and nitrogen fixation. Field observations over a seasonal time frame could be used to test hypotheses of light versus dark as developmental stages of the green berries.

References

Brock, T. and Madigan, M. 2000. Brock Biology of Microorganisms, 9th Ed. Prentice Hall. Upper Saddle River, NJ.

Dephilippis, R., Margheri, M., Pelosi, E., and Ventura, S. 1993. Exopolysaccharide produced by a unicellular cyanobacterium isolated from a hypersaline habitat. J. of App. Phycology. 4: 387-394.

Schneegurt, M., Sherman, D., and Sherman, L. 1996. Composition of the carbohydrate granules of the cyanobacterium, Cyanothece sp. Strain ATCC 51142. Arch. of Microbiology, 167: 89-98.

Shah, V., Ray, A., Garg, N., and Madamwar, D. 1999. Characterization of extracellular polysaccharide produced by a marine cyanobacterium, *Cyanothece* sp. ATCC51142, and its exploitation toward metal removal from solution. Current Microbiology, 40:274-278.

Waterbury, J. 2002 "The *Cyanobacteria*- Isolation, Purification, and Identification." The Prokaryotes. On-line edition: http://link.springer-ny.com/link/service/books/10125/.

Figure 1. Dissecting scope image of dark green berry

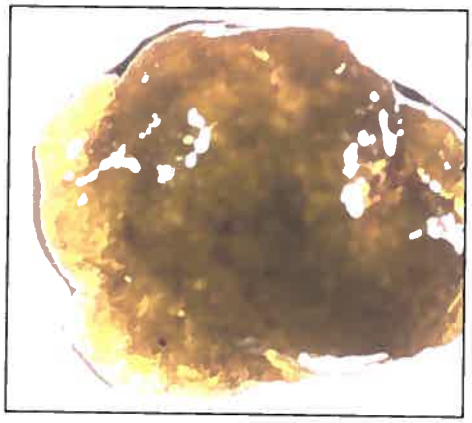

Figure 1. Dissecting scope image of light green berry

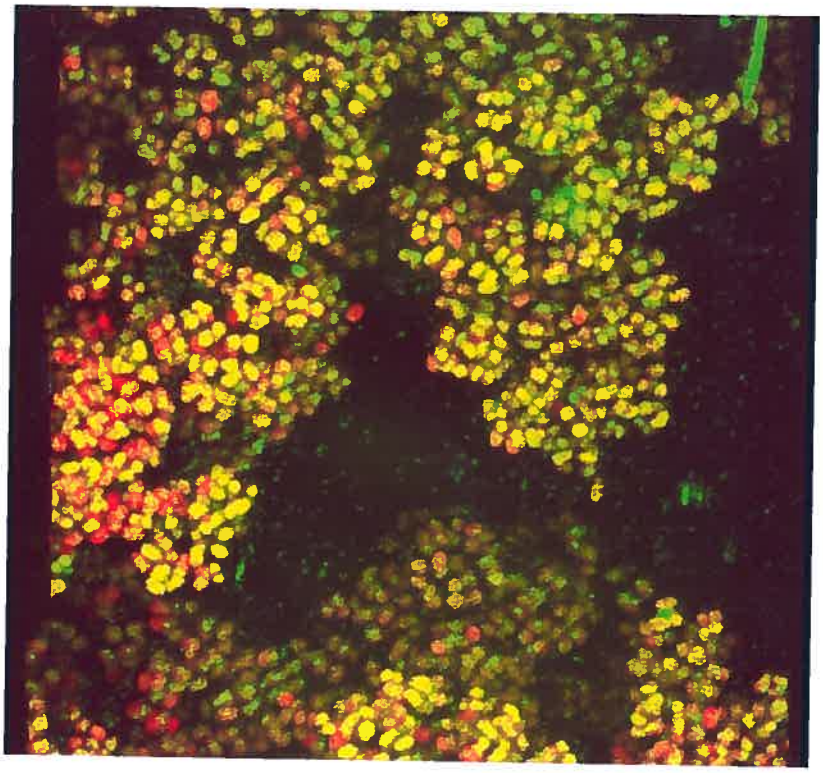

Figure 3. 40x confocal microscope image of the interior of a dark green berry

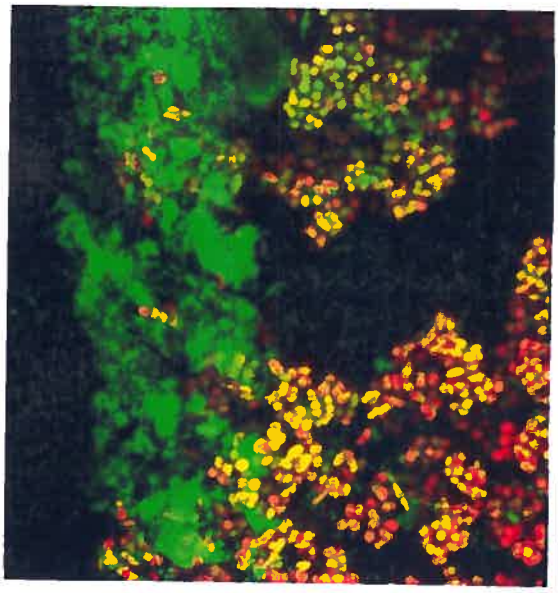

Figure 4. 40x confocal image,
Edge of a dark green berry

Figure 5. 40x confocal image,
interior of a light green berry

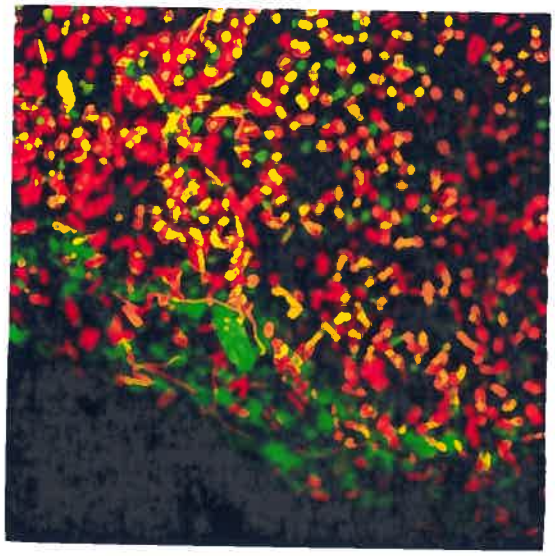

Figure 6. 40x confocal image,
Edge of a light green berry

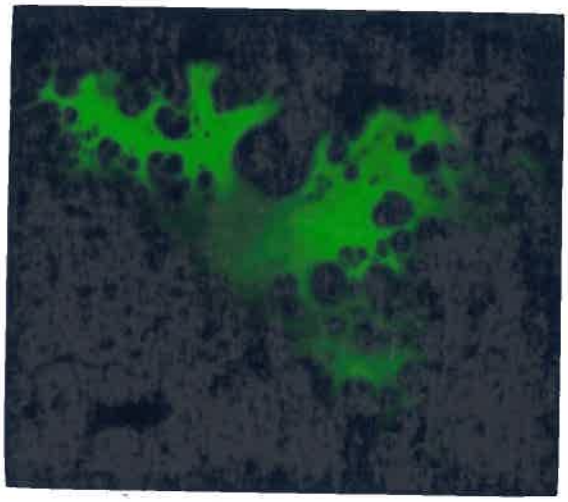

Figure 7. 40x confocal image, the matrix